Regimes of Vorticity in the Wake of a Rectangular Vortex Generator

Velte, Clara Marika; Okulov, Valery; Hansen, Martin Otto Laver

Published in:
Proceedings of PIV'11

Publication date:
2011

Document Version
Peer reviewed version

9TH INTERNATIONAL SYMPOSIUM ON PARTICLE IMAGE VELOCIMETRY - PIV11
Tsukuba, Japan, July 21-23, 2011

Regimes of Vorticity in the Wake of a Rectangular Vortex Generator

C.M. Velte[1], V.L. Okulov[1], M.O.L. Hansen[1]

[1]Department of Mechanical Engineering, Technical University of Denmark, Kgs. Lyngby, Denmark
cve@mek.dtu.dk

ABSTRACT

This paper concerns the study of the secondary structures generated in the wake of a wall mounted rectangular vane, commonly referred to as a vortex generator. The study has been conducted by Stereoscopic PIV measurements in a wind tunnel and supplementary flow visualizations in a water channel. The results show that the vane produces not only the anticipated primary vortex, but at least five vortex structures. Further, the vorticity map can be subject to various regimes, showing a dependency on the circulation of the primary vortex and the height of its center above the wall.

1. INTRODUCTION

The motivation of this work is to detect and understand the secondary vortex structures generated around a rectangular vortex generator. It is of importance to understand the regimes for secondary vortices accompanying the primary one for the fundamental understanding of the flow as well as the aspects of application (e.g., trailing vortices in aircraft wakes, wind turbine wakes, vortex generator wakes etc.).

Research on secondary vortex structures produced by streamwise vortices in ground interaction can be traced back to the work of Harvey and Perry [1], who examined the departure of the paths of trailing vortices from the ones predicted by 2D theory. The deviations were shown to be caused by the appearance of a secondary vortex in the form of a separation region obtained by the adverse pressure gradient produced by the trailing vortex. Further downstream, they also observed rapid growth of the bubble, eventually resulting in detachment yielding a free discrete vortex in addition to the continuously generated separation bubble. Fundamental work on two-dimensional cases, where these effects are also shown, has been conducted in the form of experimental visualizations (see, e.g., Harris and Williamson [2]), computations and theory (see, e.g., Kramer et al. [3]).

The appearance of horseshoe vortices around wall-mounted blades is previously known, e.g., from axial gas turbines (see, e.g., Langston [4]), which is also applicable to vortex generators though these two flows otherwise don't bear much resemblance.

2. METHOD

2.1 Wind tunnel test

For the wind tunnel tests, the experimental setup is almost identical to that of Velte et al. [5] with the following exceptions: In the same fashion as the previous study, the angle is varied ($\beta = 9{:}3{:}54^\circ$). However, this study also includes measurements for different device heights (h=5:5:25 mm), the vane length is always set to l=2h. Further, the measuring position is located at 10h downstream of the vortex generator trailing edge.

2.2 Water channel test

The water channel is purpose built for flow visualization with low Reynolds numbers ($\mathrm{Re} \approx 400$ based on vortex generator height $h_{VG} = 12\,\mathrm{mm}$, and free stream velocity $U_\infty = 40{\cdot}10^{-3}\,\mathrm{m\,s^{-1}}$) and has optical access on both sidewalls as well as the bottom of the test section. The test section dimensions are $0.3 \times 1.5\,\mathrm{m}$, the water level being set to about 0.2 m. Screens and a honeycomb structure are found at the inlet.

A flat plate of width 0.16 m and length 0.30 m was inserted vertically into the channel parallel to the test section sidewalls. Running the channel at a velocity of $0.04\,\mathrm{ms^{-1}}$ ensured a laminar boundary layer that would extend well beyond the extent of the plate. The plate was placed at a distance of 0.3 m downstream of the inlet screens and 0.05 m away from the test section wall, resulting in a distance of 0.25 m between the opposing test section wall and the plate on the side which the vortex generator is attached. A mounting system for a vortex generator, allowing for varying the angle, was incorporated as to position the vortex generator at channel mid-height at 7.5 cm from the plate leading edge.

The dye visualizations were performed using gravity feed of water solutions of food coloring dyes through hypodermic needles. The dye was kept in small containers connected to the needles by flexible plastic tubing. Matching of the speed of the exiting dye to the surrounding fluid to minimize disturbances was done by adjusting the height of the containers.

3. RESULTS AND DISCUSSION

3.1 Flow topology observations from visualizations - basic vortex system

From the dye visualizations, the flow topology of the primary vortex and the expected horseshoe vortices (c.f., Langston [4]) could be visualized and is reproduced in the sketch in Figure 1. Each vortex is indicated in the figure where *P*, generated at the upper edge of the plate in the form of a vane (wing) tip vortex, is the primary vortex. H_P and H_S are the pressure side and suction side horseshoe vortices, respectively. The pre-knowledge of these three basic vortices facilitates the use of dye visualizations through pigment injection, since this reveals the generation area of each vortex and therefore also the ideal dye injection points.

3.2 Local separation of the boundary layer

The secondary structure *S*, as identified in [5], seems to be generated by separation of the boundary layer due to the adverse pressure gradient imposed by the primary vortex on the wall. This can be seen in Figure 2, displaying streamwise vorticity plots for increasing angle of incidence of the vortex generator (data from [5]). As the primary vortex becomes increasingly stronger with device angle, the continuously generated separation region grows to eventually detach and form a discrete vortex.

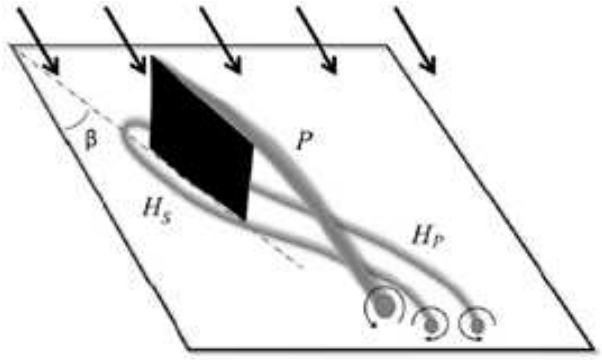

Figure 1: Topology of the basic vortex structure found from dye visualizations..

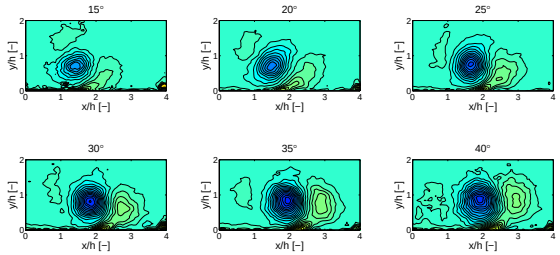

Figure 2: Generation of secondary vortex by boundary layer separation shown by increasing the angel of incidence of the vane.

3.3 *Formation of horseshoe vortices*

As is commonly observed in axial gas turbines (see, e.g., Langston [4]), the pressure distribution across the leading edge of the blade causes the vorticity lines to bend and stretch to form horseshoe vortices around the body. For the vortex generator, due to the generation of the primary wing tip vortex, the flow will appear somewhat differently. The primary vortex, P, will, at a very early stage of its generation, sweep the suction side horseshoe vortex, H_S, under it. At this stage H_S joins the secondary vorticity, S, separated by the primary vortex, which occasionally pinches off to form a discrete vortex, D, that will circuit the primary vortex, only to again later be swept in under the primary vortex a.s.o.. The pressure side horseshoe vortex, H_P, seems to evolve undisturbed by the rest of the vortex system throughout the observed downstream range. Therefore, at a far enough downstream position, the vortex system in a cross-plane will typically have the appearance depicted in Figure 3, showing an example of the measured vorticity field and a corresponding principal sketch of the vortex system.

3.4 *Regimes of the vortex system*

The adverse pressure gradient producing S should be larger if P

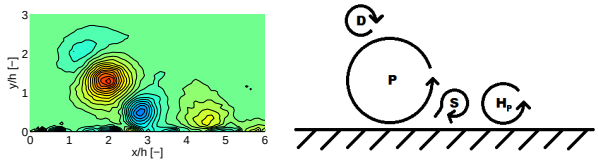

Figure 3: Typical vortex system in cross-plane downstream of vortex generator.

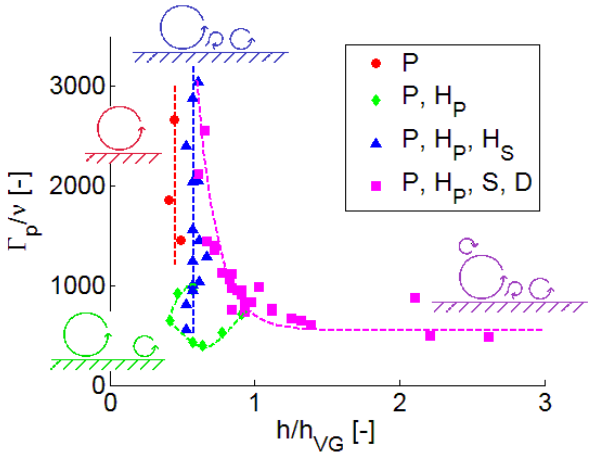

Figure 4: Regime map for the vortex system with the dependent variables circulation Γ_p of the primary vortex and its center height above the wall. The trends are indicated by dashed lines and sketches of the states are shown by figures in the graph, for clarity, both in the respective color used for the different states.

is strong and close to the boundary. It is therefore chosen to, for each of the SPIV cross-plane measurements in the parametric study, plot the circulation to the height of P above the wall. The circulation was found by integration along the vortex core radius determined from a Lamb-Oseen vortex streamwise vorticity distribution previously employed by [5]:

$$\omega_z = \frac{\Gamma}{\pi\varepsilon^2}\exp\left(-\frac{r^2}{\varepsilon^2}\right) \tag{1}$$

The results are plotted in Figure 4, where the regimes of the vortex system are indicated by: ● only P vortex present, ♦ P and H_P, ▲ P, H_P and H_S/S and ■ P, H_P, S and D. These states are also depicted by figures and indicative lines in the graph with color corresponding to the ones of the respective symbols, for clarity. For large values of the circulation, the states converge to a narrow band corresponding to a vortex center height $h/h_{VG} \approx 0.6$. In this regime, the secondary structures, which are relatively weak in comparison to P, do not affect the path of P significantly. As the circulation decreases, the narrow band bifurcates into three branches. One state, ♦, comprises P and H_P and seems to follow a complex pattern. At slightly larger distances from the wall the combined effects of H_S and the secondary vortex S appears, ▲, apparently isolating this complex effect by creating a buffer region with a relatively weak structure (H_S/S), making P non-susceptible to perturbations from H_P.

In the last regime S has grown large enough to form the detached vortex D, indicated by ■. This complex vortex pattern shows a seemingly exponential dependence between the circulation and vortex centre height, where the height increases rapidly as the circulation of P diminishes. The circulation of H_P is only weakly affected by the vane height and angle. Therefore, as S becomes increasingly stronger it will have the largest impact on P. The effect of S, having reversed sign of vorticity as compared to P, will create an upwash pair together with P, causing its motion away from the wall. This is confirmed from the vorticity maps computed from SPIV measurements for the smallest vanes. This is why the secondary vortex appears only when P is at larger distances from the wall: at an earlier stage more upstreams S has caused P to move away from the boundary by induction.

4. CONCLUSIONS

Flow visualizations and Stereoscopic PIV measurements have shown that a rectangular vortex generator produces not one, but (at least) five vortex structures, contrary to the classical misconception which assumed merely one, *P*. This last assumption has shown to be valid only under strict conditions for high circulation and where the vortex is close to the wall. The primary vortex generates a secondary vortex by local separation of the boundary layer, which may produce a discrete vortex under appropriate conditions. In addition, two horseshoe vortices are produced by vortex stretching around the generator leading edge near the wall.

Depending on the state of the measured vortex system in one cross-plane downstream of the generator, the flow can be divided into separate regimes as a function of the circulation and height of the primary vortex center. The secondary vortices have a distinct impact on the primary vortex path as the circulation decreases, whereas for large circulation these effects are substantially reduced.

ACKNOWLEDGMENTS

This work formed a portion of the Ph.D. dissertation of CMV, supported by the Danish Research Council, DSF, under grant number 2104-04-0020, and currently by EUDP-2009-II-grant Journal number 64009-0279, which are both gratefully acknowledged. Further, the authors are grateful to Dr. Robert Mikkelsen, DTU, for valuable discussions and help with practical problem solving.

REFERENCES

[1] Harvey J.K., Perry F.J. (1971) Flowfield produced by trailing vortices in the vicinity of the ground. AIAA J. **9**, 8, 1659-60.

[2] Harris D.M., Miller V.A., Wiliamson C.H.K. (2010) A short wave instability caused by the approach of a vortex pair to a ground plane. Physics of Fluids, **22**, 091106.

[3] Kramer W., Clercx H.J.H., van Heijst G.J.F. (2007) Vorticity dynamics of a dipole colliding with a no-slip wall. Physics of Fluids, **19**, 126603.

[4] Langston L.S. (2001) Secondary flows in axial turbines – A review. Annals of the New York Academy of Sciences, **934**, 11-26.

[5] Velte, C.M., Hansen, M.O.L., Okulov, V.L. (2009) Helical structure of longitudinal vortices embedded in turbulent wall-bounded flow. Journal of Fluid Mechanics, **619**, 167-177.